Identification and correction of radiative transfer modelling errors for atmospheric sounders: AIRS and AMSU-A

Philip D. Watts and Anthony P. McNally

European Centre for Medium Range Weather Forecasts, UK

Summary

This paper briefly demonstrates observed biases of measured AIRS radiances with respect to the ECMWF forecast model. The weight of evidence suggests that most of the observed bias and its variation with airmass can be attributed to errors arising from radiative transfer modelling (RTM).

Although RTM errors are potentially complex and dependent on many factors, it is shown in the paper that a simple model of the error, based on an adjustment to the channel absorption coefficient, can be estimated and the result used to considerably improve global and airmass dependent biases in AIRS data.

Departures of measured brightness temperatures from the ECMWF NWP model predictions are compared to departures expected from the simple absorption coefficient error and an optimal estimator is used to obtain values of a two parameter bias model: $[\delta,\gamma]$ where δ is a global constant and $(\gamma-1)$ is the fractional error in layer absorption coefficient.

Assimilation experiments for AIRS using $[\delta,\gamma]$ show that the air-mass dependency is effectively removed for significant parts of the observed spectrum and forecast skill scores are subsequently improved.

We discuss the seasonal stability of the modelled errors and some anomalies found in their estimation.

1. Introduction

Assimilation systems for Numerical Weather Prediction (NWP) models are based on the assumption that data are unbiased with normally distributed errors (Daley, 1993). The assimilation process requires that the NWP model state can be mapped to the observation; this mapping is termed the observation operator. In the case of remotely sensed satellite sounding data, namely top of atmosphere radiances, the observation operator is a complex radiative transfer model (RTM). The RTM calculates the interaction of radiation with the absorbing gases within the atmosphere and thus requires an accurate assessment of the constituent gas concentrations and the efficiencies with which the gases absorb and emit radiation. (Important gases with *variable* concentration are part of the NWP model 'state', e.g. water vapour or ozone, in which case their accuracy results from the assimilation process and is not an absolute requirement prior to it). Although a great deal of effort has been and is being made to refine and improve RTMs, errors of the order of 5% (Rizzi et al. 2002) remain in important sounding bands. Sources include errors in instrument channel filter response functions, in assumed (constant) gas concentrations, in line strengths, shapes, line-mixing, atmospheric layering etc. Such errors are of course not random and although neither completely constant, they usually lead to systematic errors in the top of atmosphere radiances estimated using the RTM. These errors must be corrected before the radiance data can be assimilated.

Globally constant errors are simple to monitor and correct but even a constant absorption coefficient error maps, through the RTM, into a quasi-random error. For example, if the absorption coefficient of an important absorbing gas for an instrument channel is overestimated then the RTM will erroneously calculate too high a level in the atmosphere for the origin of radiance in that channel; the *weighting function* will be too high. If the weighting function is within the troposphere this will lead to an *underestimation* of the channel radiance since the emitting temperature decreases with altitude according to the local *lapse rate*. The lapse rate is not a constant, being highest (fastest decrease) in the tropics/unstable conditions and lowest at high latitude/stable conditions. Thus the RTM error will vary according, somewhat simplistically, to the local lapse rate. 'Systematic' errors are therefore air-mass dependent.

Operational schemes to correct 'systematic' radiance errors often use regressions employing air-mass type predictors (Harris and Kelly, 2000, McNally et al., 2001). In this way, the mapping of absorption coefficient error by the RTM can be seen to be modelled by relating the error to the local lapse rate.

In this paper we firstly in section 2 describe the observed biases and their supposed atributable causes. We then explore whether it is possible to more directly identify and model the absorption coefficient error. Firstly in section 3.1 we show that a fixed error in channel averaged absorption coefficient can be modelled as an adjustment made to level transmittances in the form of an exponent γ where $(\gamma - 1)$ represents the fractional absorption coefficient error. We then introduce a bias model $[\delta,\gamma]$ where δ is a global constant that can be interpreted as the global average values of all bias contributions not attributable to simple absorption coefficient errors (for example a calibration error). Use of an absorption coefficient adjustment is not new. Turner, 1994, used it to account for CO_2 mixing ratio changes in a fast model for the High-Resolution Infrared Sounder (HIRS). Rizzi and Matricardi, 1998, also apply the technique to HIRS data analysis estimating the γ values by minimising the standard deviation in measured minus calculated brightness temperatures.

Section 3.2 defines a indicator of the air-mass dependency of an error which is useful in quantifying how well it is corrected. In section 3.3 we describe the estimation of the parameters $[\delta,\gamma]$ from observations using a simple optimal estimator and in section 4 we detail the resulting estimates for selected channels from the two satellites. In section 5 we give the results of assimilation experiments using the AIRS instrument (Aumann and Chahine, 2003). Section 6 concludes and discusses results obtained but not detailed in the paper: the effect of seasonal variations, assimilation results with AMSU-A and attempts to improve the AIRS $[\delta,\gamma]$ estimates with higher data volumes.

The RTM used in this study is version 6 of the fast model RTTOV (Saunders et al. 1999). The fast model coefficients are computed from GENLN2 (Edwards 1992) line-by-line model calculations using HITRAN 96 (Rothman et al. 1998) spectroscopic parameters and instrument characteristics released by the AIRS Science Team on 18th August 2002.

2. Observed biases

Biases observed in the AIRS measurements are globally and temporally very stable. Successful assimilation of AIRS data was achieved (McNally et al. 2004) using a globally constant bias adjustment obtained from a single month of observations.

Figure 1 shows, for AIRS channels in the spectral region 640 to 1600 cm^{-1}, a comparison of observed biases and biases found in the CAMEX experiment where HIS interferometer data were compared to GENLN2 calculations made using detailed *in situ* observations of atmospheric humidity and temperature. The CAMEX results are independent of any ECMWF forecast model biases but show a broad agreement with the AIRS biases. Similar agreement is found in the shortwave region (not shown).

Most biases can be attributed to known weaknesses in knowledge of either line strengths, line mixing or continuum absorption. Some can be tentatively attributed to errors in a gas concentration assumed in the RTM (e.g. N_2O). NWP model biases can only be proposed with any certainty in the case of the stratospheric channels (e.g. 640-690 cm^{-1} in Figure 1) where other satellite data provide corroborating evidence.

Figure 2 and Figure 3 show the globally average AIRS bias as monitored against the ECMWF model and make an attempt to attribute the bias to a cause. As we suspect that most biases are a result of weaknesses in the RTM, we now make an attempt to model the bias in terms of a simple spectroscopic error.

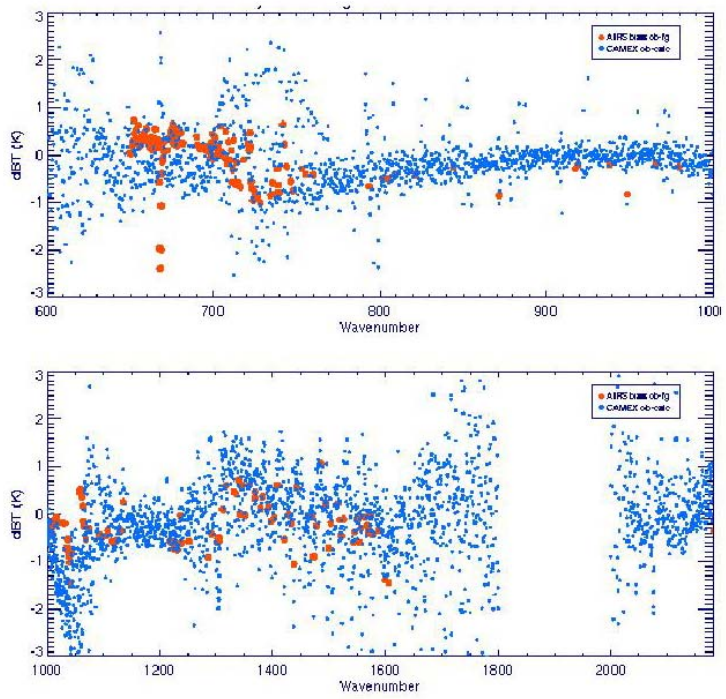

Figure 1. CAMEX (blue) and operationally monitored AIRS biases (red) from 600 to 2300 cm-1.

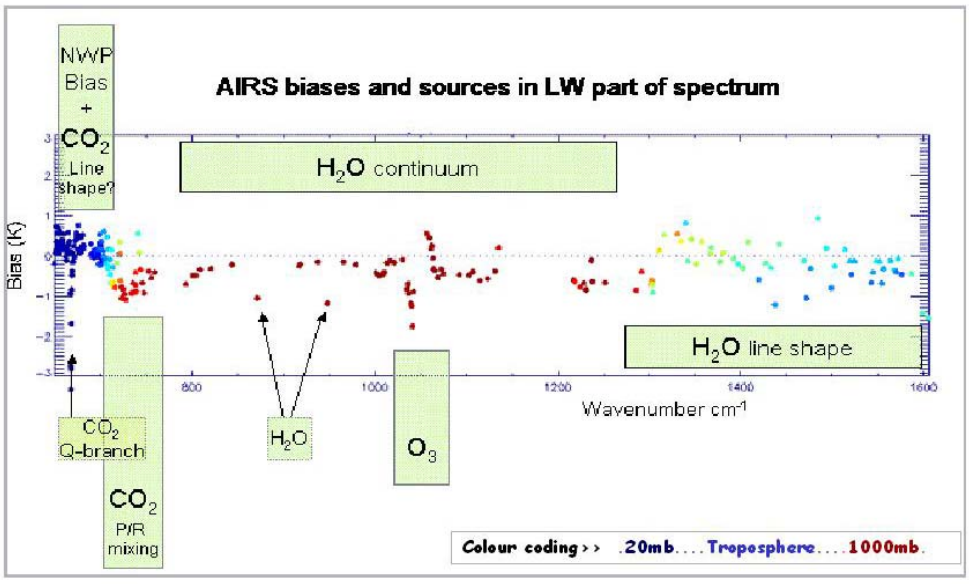

Figure 2. Biases in AIRS observations from 640-1600 cm-1and suggested attribution.

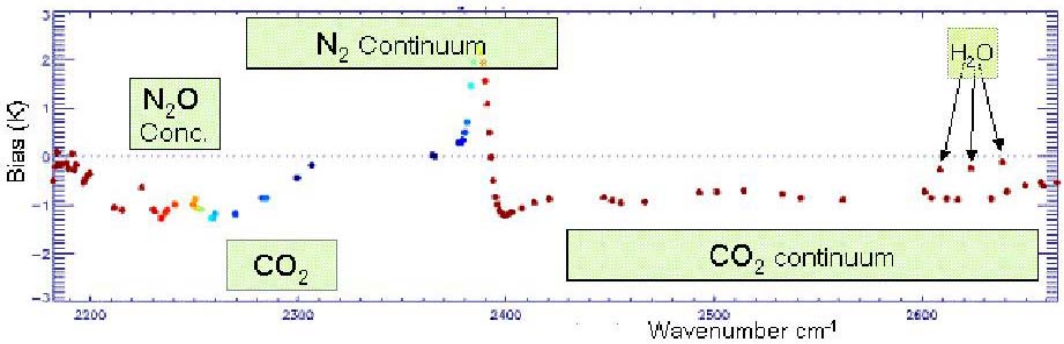

Figure 3 Biases in AIRS observations from 2180-2660 cm-1and suggested attribution.

3. Modelling the error

3.1. Modelling absorption coefficient errors

The atmospheric contribution to the top of atmosphere radiance, R_a, in channel l of a passive thermal sounding instrument can be written,

$$R_a^l = \int_{ps}^{0} B^l(T(p))d\Gamma^l(p) \quad 1$$

where $B^l(T(p))$ is the planck function (integrated over the spectral response function (SRF) of channel l) evaluated at the temperature T of the atmosphere at pressure p. This is the polychromatic approximation where B is assumed constant over the bandwidth of the channel or, alternatively, calculated using an empirically adjusted temperature T(p). p_s is the surface pressure and $\Gamma^l(p)$ is the channel transmission from level p to space defined as

$$\Gamma^l(p) = \exp-\left\{\int_{p}^{0} \kappa^l(p)\rho(p)dp\right\} \quad 2$$

where κ^l is the channel integrated absorption coefficient and ρ the absorbing gas density. We now introduce a constant fractional error γ^l in the absorption coefficient such that the true κ^l_t is related to the modelled κ_m by

$$\kappa_t^l = \gamma^l \kappa_m^l \quad 3$$

If we make the assumption that the fractional error is constant (i.e. independent of level and state of the atmosphere) we can write the transmittance as

$$\Gamma^l{}_t(p) = \exp-\gamma^l\left\{\int_{p}^{0} \kappa^l{}_m(p)\rho(p)dp\right\} \quad 4$$

or therefore

$$\Gamma^l{}_t(p) = \Gamma^l{}_m(p)^{\gamma^l} \quad 5$$

The surface contribution to TOA radiance for a surface with emissivity ε_s, is

$$R^l{}_s = B^l(T_s)\Gamma^l(p_s)\varepsilon_s \quad 6$$

showing the effect of the absorption coefficient error here can be modelled in the same way as for the atmospheric contribution.

Note that a constant fractional error in the assumed concentration ρ(p) has exactly the same functional behaviour. Less obvious is that as κ^l is the channel integrated absorption coefficient, an error in the definition of the channel SRF also has an equivalent effect. In fact errors in ρ and the SRF are more rigorously modelled in this way whereas κ^l is generally (and especially in the infra-red) a result of complex processes: temperature and pressure dependent line absorption by several gases. The error in κ^l is therefore not expected to be independent of atmospheric conditions and not even constant throughout the portion of the atmosphere relevant to a particular channel. This complexity represents a potential significant limitation of the correction method especially for the infra-red AIRS instrument. We do observe though, that biases in the *both* instruments generally have air-mass dependent contributions that are *smaller* than the global value. It seems

likely then, that the first-order effect is a simple shift of the weighting function from first-order error in κ^l, lending support to the premise of this work.

The total radiance error originating from a constant absorption coefficient error modelled by γ can therefore be succinctly written (forthwith omitting the channel index *l*) as

$$\varepsilon(\gamma) = y(\gamma) - y(1) \qquad 7$$

where $y()$ represents the full radiative transfer equation.

It would be possible to equate the ε(γ) of equation 7 with global or regionally observed biases, b[1], in the measurements compared, in our case, to the ECMWF model background values. However, we may express b as a combination of sources;

$$b = b_{abs} + b_{nwp} + b_{calib} + ... \qquad 8$$

where subscripts *nwp* and *calib* refer respectively to biases in the NWP model and channel calibration and the dots imply other error sources. b_{abs} is the bias resulting from an absorption coefficient error. We wish to equate ε_γ to b_{abs} since this is the only part we expect γ to model. It may be desirable to correct the other bias sources (and certainly is for calibration errors) but it should not be done with γ since, as discussed, this would lead to an air-mass dependence totally inappropriate to the error source. To achieve this we introduce a globally constant bias term, δ, into our bias model which then becomes

$$\varepsilon(\gamma) + \delta \cong b_{abs} + b_{nwp} + b_{calib} + ... = b \qquad 9$$

That is, the observed bias, b, is a combination of error sources that we model with a constant absorption coefficient error and a constant brightness temperature error. It is the air-mass dependence of ε(γ) that permits us to obtain estimates of δ and γ, with some degree of independence, from a large set of realisations of b.

3.2. 'Air-mass index'

In this section we devise a simple index to quantify the air-mass dependency of systematic errors. Since we suppose that a major factor is the temperature lapse rate in the region of a channel's weighting function, then we may expect significant differences in observed biases in extra-tropical and tropical regions: tropospheric lapse rates in the tropics are generally larger than those in midlatitudes. We therefore define the air-mass index (AI) as

$$AI = \frac{1}{2}\left(\overline{b_{20-90N}} + \overline{b_{20-90S}}\right) - \overline{b_{20S-20N}} \qquad 10$$

where the bars indicate means over the regions denoted by the subscripts. If we examine this quantity for a sample of AIRS data (details of which are given in section 3.2) we obtain the plots in Figure 4. The selected channels all peak in the upper troposphere and the tropical biases are shown in the top panel. The lower left panel shows the observed AI as a function of the tropical bias and, for comparison, a simulated AI obtained assuming γ=1.05 for all channels and using AFGL midlatitude and tropical profiles to characterise the atmospheres.

---

[1] The bias b is defined as the mean difference between measured radiances and radiance calculated from the NWP model state using the RTM: $b = \overline{R_{meas} - RTM(nwp)}$.

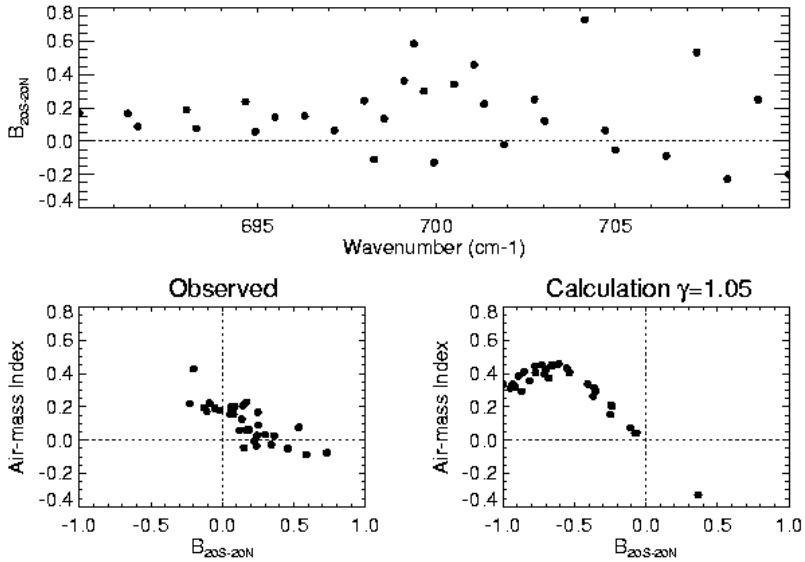

Figure 4. Observed and modelled AI values for AIRS channels in the wavenumber region 690 - 710 cm^{-1}.

Of course we do not expect the lower right plot to equate to the lower left since the channel errors do not equal +5%, but the interesting characteristic of the simulated biases is the quasi-linear behaviour (that is seen in other wavebands as well as in this restricted channel selection). Since the effect of γ is near-linear and, by definition, γ=1 would give zero tropical bias and AI, each point must in practice lie somewhere on the line defined by the origin and the position for γ=1.05. The observed scatter in the left panel can be seen to be consistent with this description if the ensemble is shifted approximately +0.3 K along the tropical bias axis. One could speculate that this shift is the result of an NWP model bias or a calibration error. In any case, the results lend support to the feasibility of the [δ,γ] bias model which aims to reduce the scatter in both bias and air-mass index.

3.3. Estimating the [δ,γ] parameters

For observations of [δ,γ] we use a sampled set of departures (measurements minus NWP model brightness temperatures) from one month of operational assimilation. The departure is defined as,

$$d = y^m - y(T,Q,O,[0,1]) \qquad 11$$

where y^m is the measured brightness temperature, T,Q and O represent the NWP model atmospheric state (temperature, humidity and ozone) and the [0,1] implies the use of the uncorrected RTM.

Each observation has an associated location defined by latitude and longitude and only observations that passed cloud, rain and other quality control checks are used. In addition, we restrict the data to near nadir; this is not a fundamental restriction but one that enables us to require only nadir[2] estimates of ε(γ).

For ε(γ), we use mean ECMWF analysis fields at 5^o resolution for the same month as the observations of *b*, and run the operational RTM model (RTTOV-6, Saunders et al. 1999) with γ = 1.05 and γ = 1. As the effect of γ values so close to unity is almost linear, we then have ε(γ):

[2] In the case of AMSU-A it also avoids the problem of significant instrument scan biases which are not related to radiative transfer modelling in any way.

$$\varepsilon_{i,j}(\gamma) = \frac{\left(y_{i,j}([0,1.05]) - y_{i,j}([0,1])\right)}{0.05}(\gamma - 1) = P_{i,j}^{105}(\gamma - 1) \qquad 12$$

where the indicies *i,j* indicate the discretised position in the 5° global grid.

A constrained optimisation is used to automate the fitting of δ and γ parameters to the observed biases. Defining the cost function for a channel as:

$$J = \frac{1}{2}\sum_{m}\frac{\left(d_m - \left[\delta + \varepsilon(\gamma)_{i,j}\right]\right)^2}{\sigma_o^2} + \frac{1}{2\sigma_b^2}(x - x_b)^2 \qquad 13$$

where *i,j* are the indicies of the 5° box in which departure observation *m* is located. *x* is a vector [δ,γ] and x_b a background estimate of [δ,γ]. σ_o and σ_b are errors in the observations and background respectively and are assumed to be uncorrelated and normally distributed. A constrained background is used because if the air-mass dependency of a RTM error in a channel is quite 'flat' (e.g. window channels) the δ and γ values will be indistinguishable; the estimates can then easily diverge and compensate each other (see section 3.3.2).

3.3.1. Observation error σ_o

The error σ_o represents the error in the estimate of [δ,γ] from a single departure observation and we can identify four contributions:

$$\sigma_o^2 = \sigma_m^2 + \sigma_{nwp}^2 + \sigma_\varepsilon^2 + \sigma_{bM}^2 \qquad 14$$

where, for each channel, σ_m is the measurement (instrument) noise, σ_{nwp} is the NWP model error (mapped into measurement space), σ_ε results from variability lost by representing the spectroscopic error as a monthly mean 5° resolution and σ_{bM} represents the forward model (i.e. bias model) error.

σ_m is the easiest term to estimate; figures could be taken from the instrument characterisation and it is reasonable to assume zero correlations.

The NWP model error σ_{nwp} could be estimated from the model B matrix and channel jacobians (i.e. $\sigma_{nwp} = HBH^T$) and the magnitude would probably be a reliable estimate. By taking sparsely sampled observations over a relatively long time period we can minimise correlations but persistent model biases cannot be avoided.

The contribution of σ_ε cannot be known until the estimation procedure is complete and even then is a relatively complex function of the variability of the atmosphere within the sampled monthly 5° box. Because this variability would affect all channels in varying degrees, a high degree of correlation can be expected.

Finally the forward model error σ_{bM} is probably the least tractable. Our knowledge of the structure and origin of the observed bias is poor and our knowledge of the inadequacy of the simple model is correspondingly poor.

Given all this, it is clear that even a crude estimate of σ_o is a tough problem; we can guess at magnitudes but the correlations are probably the crucial factor. Therefore, a pragmatic solution is chosen and σ_o is based on the observed standard deviation of the observation departures, σ_{obs} , which contains the contributions σ_m and σ_{nwp} but neither σ_ε nor σ_{bM}. A factor of 2 is used to crudely include the latter terms; $\sigma_o = 2\sigma_{obs}$.

It is worth noting that the problematic estimation of some errors outlined above disappear if δ and γ are estimated within the assimilation system. They are then treated as additional model state variables (e.g. see

Dee et.al.). In this case, because the full model state is updated there is no σ_{nwp} to account for in the observed departure. Similarly, time and space averaged model fields are not used and thus there is no σ_ε term. σ_{bM} however, remains. A potential disadvantage of this approach is that data selection (sections 3.1, 3.2) to avoid, for example, areas with NWP model biases, are general and cannot be made for the bias parameter estimation alone. A framework for this approach to bias correction in general is currently being developed at ECMWF.

3.3.2. Background error σ_b

There is no real prior estimate of $[\delta,\gamma]$, except that we expect values to centre around [0,1], and we use the background to prevent undesirable compensation effects in some channels. We therefore choose σ_b more to provide a stable minimisation than an accurate error analysis; a value of [1, 0.01] is used. These values are set empirically to give a reasonable balance with σ_o using the following reasoning.

The constraint should not force a poorer overall description of the bias than a globally fixed value. This is avoided if $[\delta,\gamma]$ is only constrained strongly in one direction; then in the poorly determined (e.g. flat $\varepsilon(\gamma)$) case where J is a long "trough", the solution still gives a lowest value of cost. We choose to apply the weak constraint to δ and the stronger constraint to γ since we a) do not wish to suggest large RTM errors where there is no strong evidence for them and b) consider that it is 'safer' to use a δ where there is no advantage in a modification to the RTM. The value of 0.01 (1%) appears low since transmission errors of typically 5% are expected. In fact, the low value is required to prevent the estimation of larger RTM errors and is a direct result of the poor modelling of σ_o. Probably it is a choice between an artificially large σ_o to account for un-modelled correlations or a correspondingly small σ_b.

3.3.3. Solution error

The theoretical error in the estimates of $[\delta,\gamma]$ is available through the inverse of the Hessian matrix (the second derivative of J). We find that the estimates are very low - they suggest very high accuracy - which is a further consequence of the inadequate modelling of σ_o, and we do not report on them in detail here. Relatively, channels with low data coverage (e.g. cloud affected AIRS window channels), high σ_{obs}, or weak dependence of the error on air-mass, show higher estimation errors, but they are not realistic (as gauged, for example, by the sensitivity of results to slightly different background constraint). We therefore had to decide on the reliability of the estimates by other means: the degree by which the AI (section 3.2) is reduced and forecast skill scores in assimilation experiments.

4. Results

4.1. NOAA AMSU-A channel 8

Sampled data and model mean profiles used for the analysis of the AMSU-A instruments (ref) were taken from 20030901 to 20030930 providing a global sample of around 400,000 soundings. Fields of view from +/-5 either side of nadir are taken and cloud or rain contaminated data are avoided.

As an example of the process we show in Figure 5(a) the observed bias (mean departure) field, (b) the modelled bias field ($\delta + \varepsilon(\gamma)$, where δ = 0.55, γ = 1.0313) and (c) the residual bias (observed minus modelled) for NOAA-15 AMSU-A channel 8.

It is clear from (a) and (b) that the main structures of the global bias field can be explained by a absorption coefficient error of +3.1% and the 0.55 K global offset although certainly there is significant detail that is not reproduced.

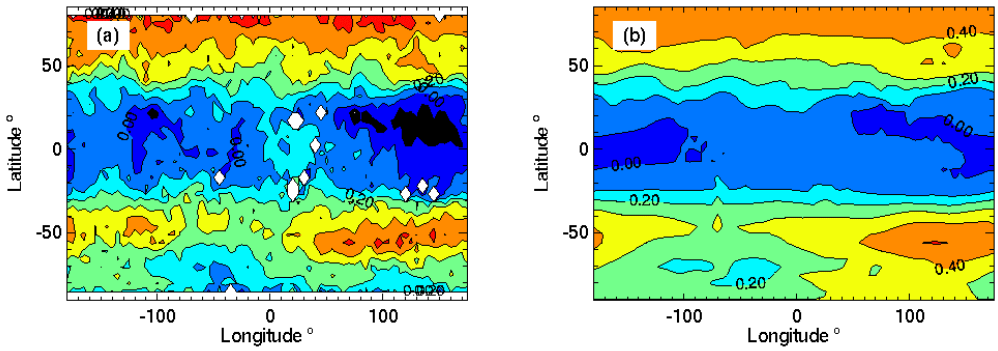

Figure 5. Estimation of [δ,γ] for NOAA-15 AMSU channel 8. (a) observed bias, (b) modelled bias. All plots are global, on a 5° grid and scaled -0.1 to +0.4K (blue to red).

The features that are present are sufficiently distinctive that it seems unlikely that other error sources (e.g. systematic NWP model error) can be responsible for them. Significant features remaining in the residual field are small and unexplained.

We find that the [δ,γ] model has a skill similar to that of channel 8 for the other lower sounding channels of AMSU-A (channels 5-7) but a poor for the higher sounding channels (9-14) where NWP model error becomes large.

4.2. AQUA AIRS

Sampled data used for the analysis of AIRS biases were taken from 20030801 to 20030830. Every 20th sounding was selected provided that the absolute departure in the AIRS channel 787 (10.89 μm window) was less than 5.0 K. This provided a global sample of around 40,000 soundings with a relatively high proportion of clear window channels compared to an unfiltered set. To avoid unacceptable contamination by NWP model errors the following additional filtering is made depending on the channel characteristics as follows:

- Winter pole stratopause errors: channels with[3] $P_{peak} < 70$ mb use latitude range [40°S-90°N]
- Model surface temperature errors: channels with brightness temperature sensitivity to skin temperature, $\delta BT_i/dT_s > 0.2$ use ocean data only.
- Avoiding non-LTE and surface reflection: channels with $\lambda < 4.58$ μm use only night-time data.

Cloud contaminated measurements are avoided using the flags set by the detection system within the operational assimilation (McNally and Watts, 2003).

Figure 6 shows the resulting estimated [δ,γ] values in the wavenumber region 650 to 1000 cm^{-1} encompassing the 15 μm CO2 sounding band through to the 11 μm atmospheric window. Error bars are drawn in exaggerated fashion (six times the estimated standard deviation) so that the relative accuracy in different channels is readily apparent. Estimates are predicted to be most accurate for channels in the 700

[3] A convenient measure of the effective altitude of a channel, P_{peak} is the temperature jacobian weighted mean pressure.

cm-1 region which sound the upper troposphere / lower stratosphere where data coverage is good and measurement noise low.

Lowest accuracy is predicted in the window region because of low cloud-free data quantities and in the higher stratosphere because of higher measurement noise. The channels at wavenumbers 871.3 and 948.2cm^{-1} are of interest because the scheme predicts large absorption coefficient errors (γ = 1.056 and 1.089, respectively). Subsequent changes to the line-by-line modelling of water vapour at these wavelengths (Rizzi, Matricardi et al.) have since improved biases in these channels. Figure 7 shows data from the CAMEX experiment (Matricardi, pers comm.) where HIS airborne interferometer data were compared to Genln2 calculations made using *in situ* atmospheric profiles. More strongly absorbing HIS channels appear as outliers in the distribution and two channels which correspond closely to the AIRS channels under discussion are marked with larger dots. The triangles show, for these channels only, the improved fit with the revised spectroscopy. A quantitative comparison of the transmittance change with the estimated γ is not possible since the channel spectral response functions are not strictly matched, however, it is clear that the revised spectroscopy makes the transmittance significantly smaller (giving lower Genln2 radiances) which is consistent with $\gamma > 1$, providing an independent corroboration of the present results.

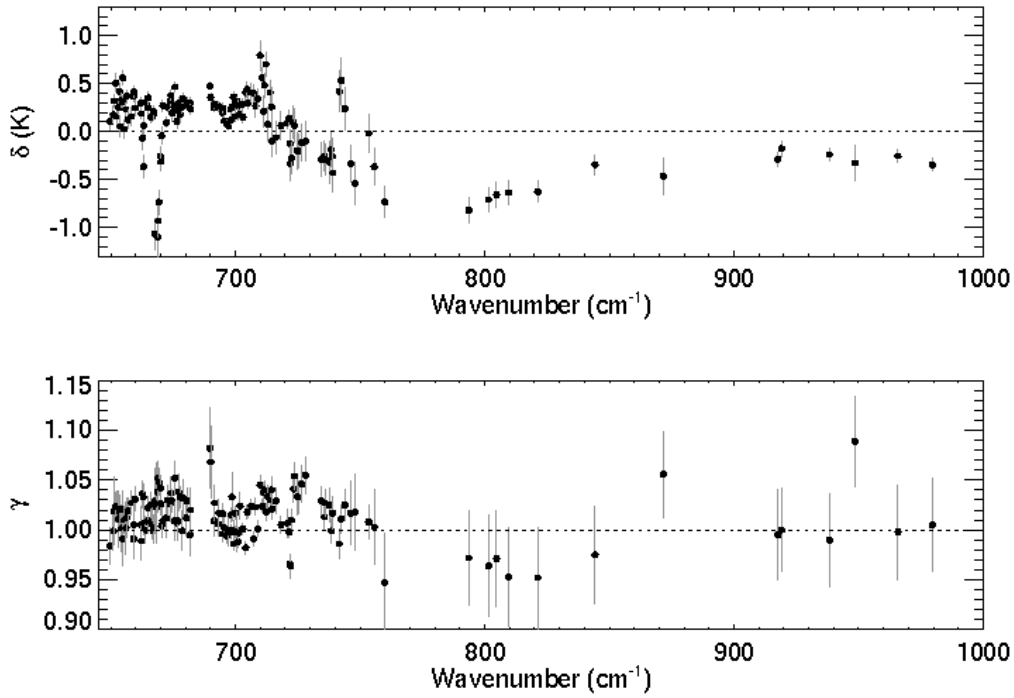

Figure 6. [δ,γ] estimates for AQUA AIRS channels in the 650-1000 cm^{-1} wavenumber region. Error bars are drawn from minus to plus six times the estimated solution standard deviation.

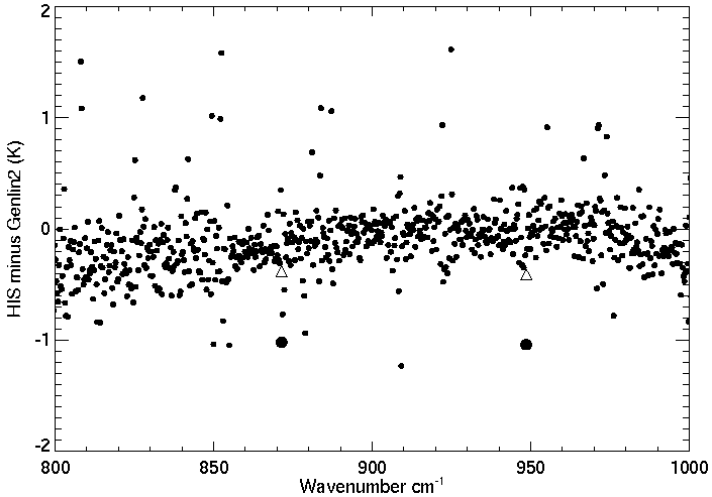

Figure 7. Comparison of airborne HIS interferometer and Genln2 line-by-line brightness temperatures. Two channels selected by the larger dots correspond approximately to the AIRS channels at 871.3 and 948.2 cm^{-1}. Triangles mark the comparison (for these channels only) after revised spectroscopy is included in Genln2.

The estimated [δ,γ] values for the sounding region are perhaps better viewed as a function of the channel peak pressure, Figure 8. Here we see a consistent positive δ of 0.2/0.3 K for channels peaking from the mid-troposphere to the high stratosphere.

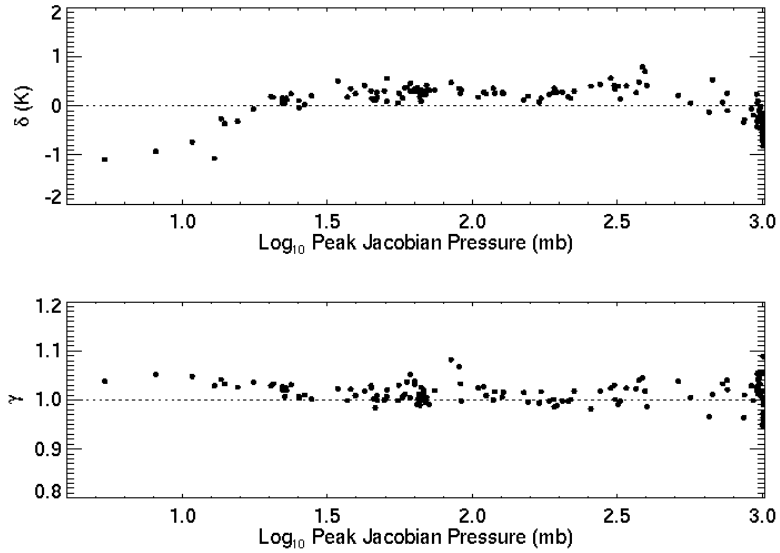

Figure 8. [δ,γ] estimates for AQUA AIRS channels in the 650-1000 cm^{-1} wavenumber region with the results plotted against channel peak pressure (log scale).

It may be that its origin is a bias in the NWP model temperature. If this is the case then a requirement that δ be smooth (in this pressure ranked space) could provide a useful constraint on the estimates. For the very highest 8-10 channels δ gradually becomes negative suggesting the influence of high level NWP biases. γ values are more evenly distributed around 1 although a slight positive bias is present. The distributions are of interest because, as discussed, δ and γ can potentially compensate each other; in the troposphere $\gamma > 1$ and $\delta > 0$ have similar global effects, in the stratosphere $\gamma > 1$ and $\delta < 0$ have similar effects. Figure 8 suggests that such a compensation is at least not a strong feature of the results since there is no systematic cross-over of estimates at around 100 mb.

The water vapour absorption band from 1150 to 1600 cm^{-1} is another important sounding region of the AIRS instrument. [δ,γ] estimates in pressure ranked coordinates for this region are plotted in Figure 9. Error bars

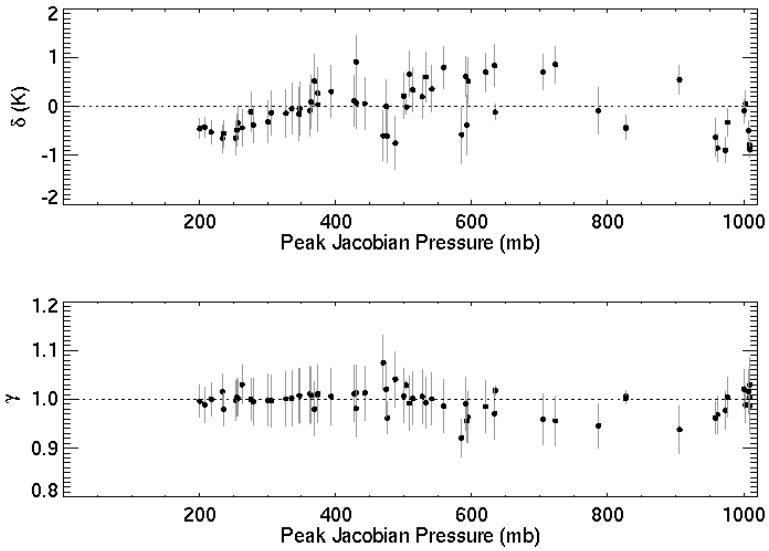

Figure 9. [δ,γ] estimates for AQUA AIRS channels in the 1150-1600 cm^{-1} wavenumber region with the results plotted against channel peak pressure.

(inflated as before) show that estimates are relatively poor compared to the CO_2 band and this is mainly because the NWP model error, σ_{nwp}, is relatively high. Observation errors in the estimation process are 3-4 times larger than for the CO_2 band. In addition, the air-mass dependence effect of absorption coefficient errors is somewhat smaller in the humidity band. Some consistency in seen in the upper tropospheric channel δs but little for lower channels. Compared to the CO_2 band more of the bias is 'explained' by the δ than the γ, and this is probably a result of the relative values of the background errors (section 3.3.2).

5. Assimilation experiments

To test the proposed bias model we performed assimilation experiments with the AIRS instrument. Northern hemisphere summer (2003/06/01 to 2003/06/22) and winter (2004/01/01 to 2004/01/22) periods were chosen and estimates of [δ,γ] from the 2003/08 period were used. For a control to the experiments, we take the operational system. It uses a globally fixed bias correction (δ', γ=1) where the δ' were

estimated from data in the period 2002/11 and which have subsequently been found to vary very little over the AQUA mission. Within the operational system around 174 of the 324 transmitted AIRS channels are used, provided they pass cloud checks. The remainder are blacklisted for various reasons. Because of solar radiation effects, 66 channels with wavenumbers greater than 2248.6 cm^{-1} are removed. 38 channels in the ozone band from 965.4 to 1230.8 cm^{-1} and 42 channels in the 15 μm sounding band which respond to very high altitudes are removed because vertical structure functions in the assimilation system transfer the measured information inappropriately.

For a detailed description of the data thinning, cloud detection, noise levels etc, for AIRS within the ECMWF 4Dvar assimilation system see McNally et al 2004.

We present here two diagnostics from the assimilation experiments to validate the [δ,γ] bias model. Firstly, the AI values which show how effectively the correction reduces air-mass dependency in the biases (section 3.2). Secondly, forecast scores which quantify the benefit obtained from using the bias model.

5.1. Air-mass Indicies

Figure 10 shows the AI obtained from the 200306 assimilation [δ,γ] experiment and the control in four bands of the AIRS instrument. In all bands, the experimental results shows reduced spread of both the tropical bias and air-mass index although the degree of improvement is variable.

The [δ,γ] bias correction is able to reduce the tropical bias as well as the AI because it is not forced to compromise between tropical and high latitude biases. Significant improvement is seen in the longwave (CO_2) sounding band (d) whereas in the other three bands, the reduction is more modest. Persistent geographical biases in the NWP model will set a minimum region to which the AI plots can collapse, and the spread in especially the humidity band (b), may be at least partially due to this. AI results for the 200401 winter assimilation experiment are similar to those for 200306 and are not shown. This demonstrates that the [δ,γ] estimates from a summer month remain valid in a winter month and supports the idea that the γ represents errors in RT modelling and not NWP model biases (although see section 5).

For the AMSU-A instruments we find that the reduction in AI using the [δ,γ] bias model is almost exactly the same (not shown) as that given by the operational air-mass regression system (Harris and Kelly, hereafter HK). There is also some evidence that the new model improves the correction in unstable tropical regions.

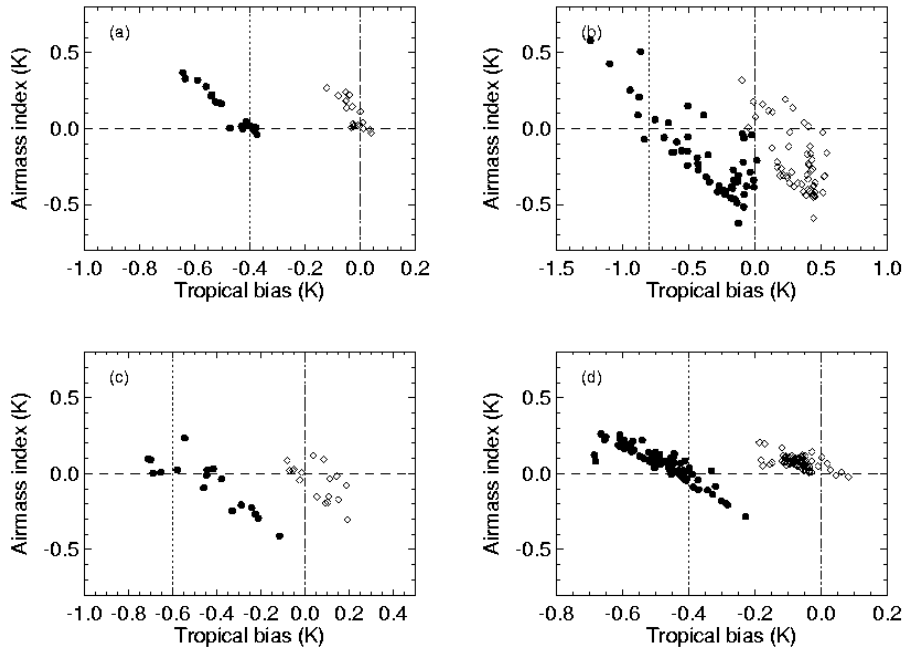

Figure 10. Air-mass indicies from the 2003/06 assimilation experiment using [δ,γ] (◊) and from the operational control (•). For clarity, control values are offset on the abscissa by the amount shown. (a) 'Shortwave' sounding channels 2181-2240 cm^{-1}; (b) humidity sounding channels 1200-1600 cm^{-1}; (c) 'window' channels 740-948 cm^{-1}; (d) 'longwave' sounding channels 650-740 cm^{-1}.

5.2. Impact on forecast performance

Forecasts have been run from the assimilation experiments using the [δ,γ] bias model and compared to the operational control.

For AIRS, 44 days of assimilation results from the summer and winter months were combined and the forecast accuracy verified by the operational analyses at the forecast valid time. Anomaly correlations for the

500 mb geopential height errors for the Northern and Southern hemispheres show improved mean forecast skill with the [δ,γ] bias model; the greater impact being found in the Northern hemisphere. T-tests show that the improvement in scores is significant and there are no areas / forecast periods where the new bias correction causes a significant degradation in scores.

With AMSU-A the forecast performance is generally degraded compared to the operational control which uses the HK air-mass correction scheme. Why this should be, given the positive results of the AI diagnostic (and no indication of poorer observation fits in routine statistical analyses), remains unexplained. One candidate reason is the interaction of the [δ,γ] bias model with the scan-bias correction that is required for AMSU-A instruments. An approximate adjustment was made to this correction based on the γ values and mean model atmospheric profiles but it is possible that a thorough retuning of the scan correction is required.

6. Discussion and conclusion

A simple physically based model is able to bias correct AMSU and AIRS radiative transfer calculations and convincingly reproduce the air-mass dependency of the error.

There are distinct advantages to the method. As it is physically based it does not rely on arbitrarily chosen predictors and is consequently less likely to model effects which do not arise from radiative transfer errors. The two parameters of the model should require only small amounts of data to determine them, although the presence of various error sources, particularly geographical biases, mean that use of well sampled data is prudent. Finally, there is the potential to relate the values of the parameters, especially γ, back to more fundamental error sources within the RTM.

Whatever the merits of the bias model, a requirement of it, if it is to be the operational correction system, is that it will have to be as effective as the alternatives. On this, the results from the present study are mixed.

6.1. AMSU-A

Whilst the skill of the bias model for tropospheric AMSU-A channels is visually striking and AI diagnostics are as satisfactory as the operational air-mass regression bias correction, assimilation experiments gave consistently poorer scores than the control despite some indication of better correction in unstable tropical regions. The reasons for this are not yet clear, however, they may lie in the interaction with the large scan bias correction for this instrument. For this instrument the new bias model is in comparison with an established and highly tuned correction system and cannot be considered to be at as mature a stage of development.

The seasonal stability of the estimated [δ,γ] was tested using winter and summer months and found to be good (less than 10% variation).

6.2. AIRS

At all levels of evaluation, from the AI diagnostic to assimilation experiments, the new bias model for AIRS is a considerable improvement over the operational system. However, unlike AMSU-A, here the comparison favours the new model as the operational correction is a simple global δ. We cannot at this stage therefore say that the [δ,γ] bias model is ready to replace the HK scheme; the latter method is yet to be fully applied to AIRS at ECMWF.

The seasonal stability of the [δ,γ] estimates for AIRS is also less good than for AMSU-A with variations of up to 50%. This could be for several reasons[4]. Firstly, the simplistic nature of the bias model may not follow changes in RTM errors that are very sensitive to exact conditions prevailing. Since, however, in any one month of global measurements, most climatic conditions are represented, this seems unlikely. More likely perhaps are seasonal variations in NWP model bias (particularly in ozone and water vapour) that alias into the modelled RT error. A third possibility is that the low data numbers used for AIRS leads to sampling effects[5].

Despite the caveats, the new bias model is effective and has merits that warrant further efforts to improve it. The general principle that the correction should be close to the underlying physics is one that has not, judging by the literature, been followed adequately. Global assimilation systems, although not as precise in some ways as controlled experimental conditions, do represent a huge available database to be exploited by those seeking to improve our knowledge of radiative transfer parameters.

7. References

Aumann, H. H., Chahine, M. T., Gautier, C., Goldberg, M. D., Kalnay, E., McMillin, L. M., Revercomb, H., Rosenkranz, P.W., Smith, W. L., Staelin, D.H., Strow, L.L., and Susskind, J. 2003 'AIRS/AMSU/HSB on the Aqua Mission: Design, science objectives, data products, and processing systems'. *IEEE Transactions on Geoscience and Remote Sensing* **41**, **no.2**, 253-264.

Daley, R., 'Atmospheric Data Analysis', 1991 *Cambridge University Press*, New York.

Edwards, D.P., 1992, 'genln2: a general line-by-line atmospheric transmittance and radiance model: version 3.0 description and users guide', Rep. NCAR /TN-367 +STR, National Center for Atmospheric Research, Boulder, Colo.

Harris, B.A. and Kelly, G. 2001: 'A satellite radiance-bias correction scheme for data assimilation'. *Q.J.R.Meteorol. Soc*. **127**, 1453-1468.

Liebe, H.J., 1989. 'MPM - a millimetre wave propagation model. *Int. J. Infrared and Millimetre Waves*, **10**, 631-650.

McNally, A.P., Derber, J.C., Wu, W. and Katz, B.B. 2000. 'The use of TOVS level-1b radiances in the NCEP SSI analysis system'. *Q.J.R.Meteorol. Soc*. **126**, 689-724.

McNally, A.P., Watts, P.D., Smith, J.A., Engelen, R.J., Kelly, G., Matricardi, M., Thepaut, J.N., 2004. 'The use of AIRS radiances in the ECMWF 4DVar assimilation system'. Submitted to *Q.J.R.Meteorol. Soc*. / *ECMWF Tech. Memo* tbc.

Rizzi, R and Matricardi, M, 1998. 'The use of TOVS clear radiances for numerical weather prediction using an updated forward model'. *Q.J.R.Meteorol. Soc.* **124**, 1293-1312.

Rizzi, R., Matricardi, M and Miskolczi. F., 2002. 'On the simulation of uplooking and downlooking high-resolution radiance spectra with two different radiative transfer models'. *Applied Optics* **41**, 940-956.

[4] There is no evidence that the instrument characteristics have changed significantly in this period.

[5] This was addressed by reframing the J minimisation as a sequential estimator that was applied to data volumes of order 100 times larger. The AI diagnostic was improved for window channels but poorer for all other bands. Forecast scores were also poorer although still marginally better than the control. We do not understand why the high data volume estimates give poorer results.

Rothman, L.S., Rinsland, C.P., Goldman, A. Massie, S.T., Edwards, D.P., Flaud, J.-M., Perrin, A., Camy-Peyret, C., Dana, V., Mandin, J.-Y., Schroeder, J., McCann, A., Gamache, R.R., Watson, R.B., Yoshino, K., Chance, K.V., Jucks, K.W., Brown, L.R., Nemtchinov, V., and Varanasi, P., 1998, 'The HITRAN molecular spectroscopic database and HAWKS (HITRAN Atmospheric Workstation): 1996 edition', *J. Quant. Spectrosc. Radiat. Transfer*, **60**, 665-710.

Saunders, R.W., Matricardi, M. and Brunel P., 1999. 'An improved fast radiative transfer model for assimilation of satellite radiance observations'. *Q.J.R.Meteorol. Soc*. **125**, 1407-1425.